Initial Stages of Fe Chemical Vapor Deposition onto Si(100)

D. P. Adams, L. L. Tedder,* T. M. Mayer, B. S. Swartzentruber, and E. Chason
Sandia National Laboratories, P.O. Box 5800, Albuquerque, New Mexico 87185
(Received 11 January 1995)

We study the evolution of layer morphology during the early stages of Fe chemical vapor deposition (CVD) onto Si(100) via pyrolysis of $Fe(CO)_5$ below 25 °C. Scanning tunneling microscopy (STM) shows that nuclei formation is limited by precursor dissociation which occurs on terraces, not at step sites. Also, the average size of clusters formed during CVD is larger than for Fe growth by evaporation (a random deposition process). Based on STM data and Monte Carlo simulations, we conclude that the CVD-growth morphology is affected by preferential dissociation of $Fe(CO)_5$ molecules at existing Fe clusters—an autocatalytic effect.

PACS numbers: 68.10.Jy, 68.55.Jk, 81.15.Gh

The fabrication of thin-film structures often relies upon controlling or manipulating the processes of nucleation and growth. Therefore, it is critical to have an understanding of atomic-scale events taking place during the earliest stages of deposition. In the past, most atomistic studies of thin-film morphology have focused on growth by molecular beam epitaxy (MBE) [1–5]. These investigations typically involve monitoring the temporal evolution of certain morphological features, such as islands in the submonolayer coverage regime, and kinetic processes affecting MBE growth are identified by comparing the morphology for different substrate temperatures and deposition rates. These studies have contributed greatly to the understanding of MBE. However, less emphasis has been directed at characterization of other growth techniques, in particular, the development of film morphology during chemical vapor deposition (CVD) [6–11].

It is not surprising that only a small amount of experimental work [7–11] has focused on the development of morphology during CVD, considering the complex nature of this growth technique. In conventional condensation theory, nucleation rates are limited by energetic barriers associated with the formation of critical-size nuclei, while morphology is controlled by adatom mobility [12]. In contrast, CVD may involve additional processes, which may control both formation of nuclei and the evolution of structure. Adsorption, desorption, site-specific chemical reactions, and transport can each affect film structure during CVD, depending on the deposition parameters. Furthermore, growth may involve several species including precursor molecules, adatoms, and dissociation fragments.

In this Letter, we present a study of a model CVD system: Fe deposition on Si(100) by pyrolysis of $Fe(CO)_5$. The goal of this work is to understand how various kinetic processes affect film morphology in a system controlled by chemical reactions. Using scanning tunneling microscopy (STM), we monitor the nucleation sites and make detailed measurements of the cluster density and the average cluster size as a function of coverage and substrate temperature. We identify the important kinetic processes affecting morphology by making comparisons of the CVD grown films to those grown by Fe evaporation and by use of kinetic Monte Carlo simulations.

We choose to study the pyrolysis of $Fe(CO)_5$ on Si(100) for several reasons. This reaction is known to be relatively clean, for no C or O has been detected using Auger electron spectroscopy [13,14] and x-ray photoelectron spectroscopy [15] after exposing $Fe(CO)_5$ to hot Si substrates fixed at the same temperatures used in this work. Furthermore, several key kinetic parameters have already been determined such as the activation energy for desorption of $Fe(CO)_5$ precursor molecules [16,17] and the activation energy for dissociation on an Fe surface [13]. This makes attempts to model the kinetics of growth tractable. Also, identifiable changes in the initial growth morphology are expected to develop over a range of low substrate temperatures, at which the relative rate of silicide formation may be small and the surface mobility of Fe atoms on Si should be low.

The experiments involve depositing Fe layers within an ultrahigh vacuum (UHV) system equipped with a scanning tunneling microscope [18]. Si(100) samples [*n*-type (P), 0.1–1.0 Ω cm] are annealed to 1250 °C *in situ* to remove the surface oxide and impurities. The substrates selected for subsequent deposition have less than ~10% "vacancy-type" surface defects with no evidence of extended $(2 \times n)$ defects. Before growth, the Si samples are equilibrated 1 h at a temperature below 250 °C [19]. A freshly distilled $Fe(CO)_5$ source is loaded onto the vacuum system during this temperature equilibration step. The source is freeze pumped to remove impurities and then allowed to warm to room temperature. A controlled partial pressure of $Fe(CO)_5$ is introduced into the vacuum system using a UHV leak valve. In the current work, we used one of two different pressures: 1×10^{-8} or 5×10^{-8} Torr [20]. Films are also deposited onto clean Si(100) substrates by Fe evaporation for comparison to CVD growth. The evaporation source consists of a W filament wrapped with an Fe ribbon.

Images are deemed suitable for measurement if Si dimer rows and steps are easily identified. All images analyzed in this work were taken using a sample-tip

 0031-9007/95/74(25)/5088(4)$06.00

bias of −2.5 V and a tunneling current of 0.15 nA. For the purpose of determining coverage, we assume that the bright features shown in STM images are clusters of Fe atoms. Individual atoms within a cluster are not clearly resolvable. The average cluster size measured from numerous STM images is expressed in $Å^2$. The film coverages measured using STM in this way are within a factor of 3 of quantitative measurements using heavy ion backscattering spectrometry [21].

The morphology characteristic of CVD growth at temperatures less than 250 °C is displayed in Figs. 1(a) and 1(b). These images show Si surfaces after exposure to 0.5 and 5.0 langmuir (1 L = 10^{-6} torr sec) of $Fe(CO)_5$ (substrate maintained at 215 °C). At low coverages, the morphology consists of isolated clusters distributed on Si terraces, showing no preference for nucleation at steps. The cluster nucleation rate is very sensitive to substrate temperature. In Fig. 2, we plot the cluster density versus exposure for different growth temperatures, covering a range of ~100 °C. In addition, no reaction is observed after lengthy exposures (~100 L) at 30 °C . This behavior is typical of thermally activated chemical reactions and indicates that formation of new nuclei is rate limited by dissociation of the precursor molecules on the surface. We also find that the average cluster size increases with coverage, as can be seen in a comparison of Figs. 1(a) and 1(b). The cluster density and average size remain unchanged after lengthy postgrowth anneals for all coverages; i.e., no coarsening occurs at temperatures less than 250 °C.

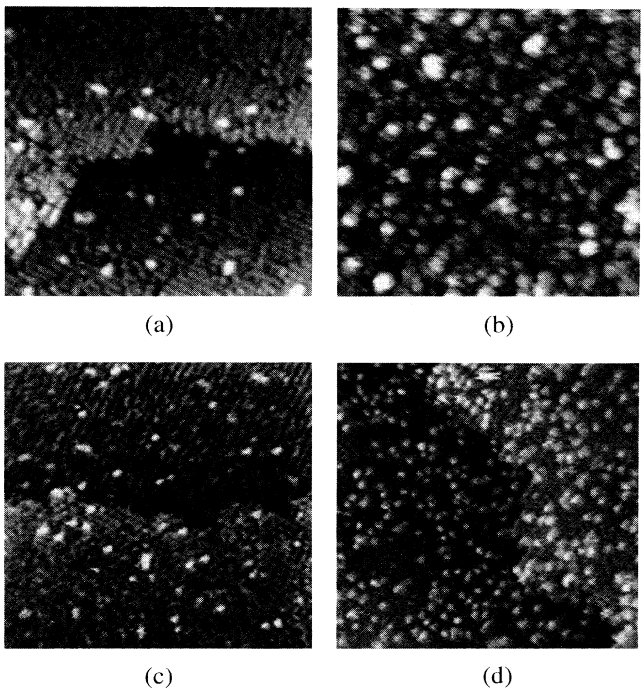

FIG. 1. 310 Å × 310Å STM images of Fe layers grown at 215 °C onto clean, reconstructed Si(100) by chemical vapor deposition [(a) and (b)] and Fe evaporation [(c) and (d)]. All images were taken using a bias of −2.5 V and a tunneling current of 0.15 nA.

In order to elucidate the role of processes that involve the chemistry of the precursor, we performed experiments in which Fe was simply evaporated onto Si(100) substrates at the same growth temperatures. In evaporation, Fe atoms are deposited randomly on the surface. As can be seen in Fig. 1, the morphology developed during evaporation is different from CVD growth. Namely, a smaller average cluster size is consistently found on samples grown by evaporation—summarized in Fig. 3. The slow increase in the cluster size of evaporated films with dose and the fact that the islands do not coarsen suggest that Fe adatoms are immobile at these temperatures.

The difference between the CVD and evaporation morphologies arises from thermally activated processes specific to the chemistry of the precursor. In particular, we find that there is a differential dissociation probability such that the precursor dissociates preferentially at an existing nucleus (an autocatalytic effect).

We have employed kinetic Monte Carlo simulations of the growth process to show that a differential reaction probability is necessary to produce large islands for CVD growth [22]. $Fe(CO)_5$ molecules arriving on top of or at the edge of an existing island, either by diffusion of a mobile precursor or by direct impingement, must have a higher dissociation probability than those precursor molecules arriving at Si substrate sites to obtain the experimentally observed structure. This is true regardless of whether or not we allow the weakly bound precursor molecules to be mobile. In the simulations we assume that the activation energy for dissociation on Si is ~3× greater [23] than the activation energy for dissociation onto a preexistent Fe cluster, previously measured to be 0.14 eV [13]. The barrier to dissociation on the Si surface used in the simulations is a rough estimate taken from the

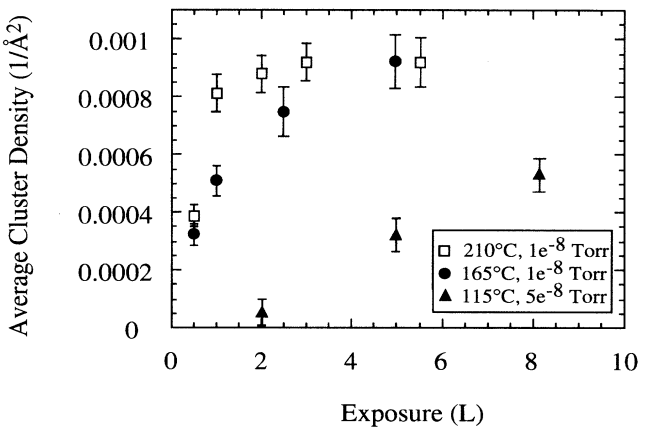

FIG. 2. Plot of cluster density as a function of exposure for three different substrate temperatures. The nucleation rate is very sensitive to substrate temperature.

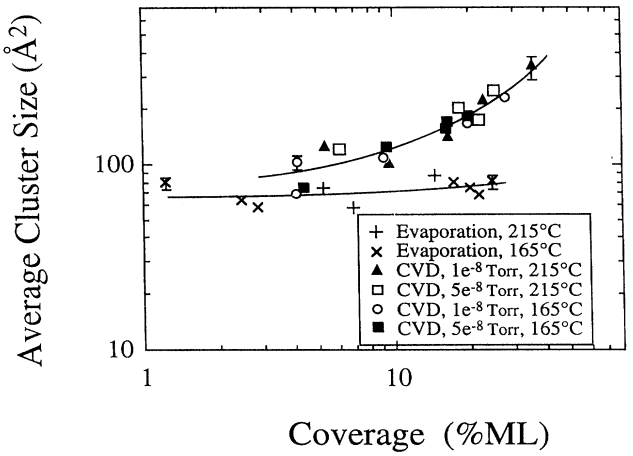

FIG. 3. Plot of the average cluster size that develops during growth by CVD vs evaporation. For equal areal coverages, a larger average cluster size develops during growth by CVD. The lines are guides to the eye. Each point is the average measured from ten images. A few error bars (characteristic of all data) are shown in the plot, which represent the scatter in average cluster size taken from different areas on the same sample.

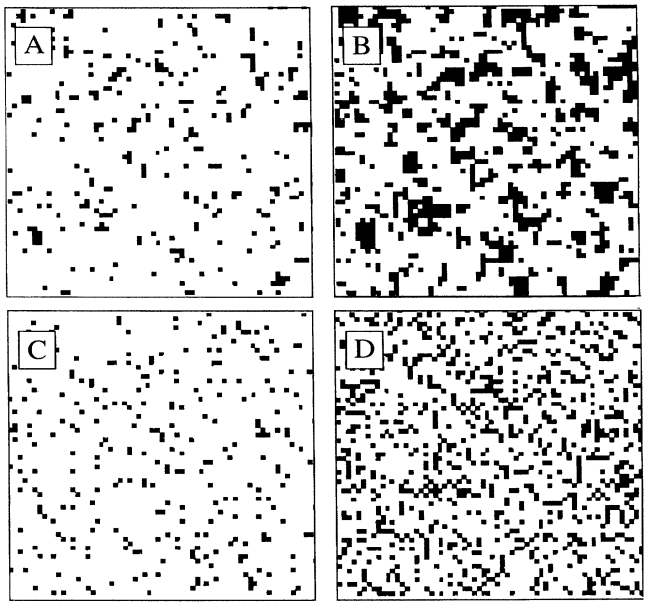

FIG. 4. Simulated CVD cluster morphology for coverages of ~0.07 and 0.25 monolayer showing the effect of differential dissociation probability [(a) and (b)] vs the effect of a uniform dissociation probability [(c) and (d)]. We assume that physisorbed precursor molecules are mobile in each. Note, (c) and (d) are equivalent to the simulated morphology for growth by Fe evaporation.

STM data. The difference in island morphology generated by preferential dissociation is shown in Fig. 4. In this figure, the island morphology at similar coverages is contrasted for the case of differential dissociation probability [Figs. 4(a) and 4(b)] with that assuming uniform dissociation probability [Figs. 4(c) and 4(d)]. The autocatalytic behavior results in an incubation period followed by rapid linear growth, as observed in bulk CVD experiments [24]. Uniform dissociation probability produces a larger density of small islands, similar to the experimental observations for Fe evaporation.

We also use Monte Carlo simulations to test for more subtle kinetic effects involving the precursor transport mechanism(s). Two different mechanisms that may affect morphology are considered. This includes transport from the gas phase and the process of molecular surface diffusion. In the first case, the precursor either dissociates upon impact, or does not stick and is simply reflected from the surface. In the second, a large fraction of physisorbed $Fe(CO)_5$ molecules diffuse and either dissociate or desorb. We consider the case for having mobile carbonyl molecules because previous thermal desorption measurements of $Fe(CO)_5$ from Si indicate an activation barrier for desorption of only 0.35 eV [17], suggesting a very weakly bound short-lived molecular precursor, with very low steady-state coverage during exposure.

In the simulations, we assume that the activation energy for surface diffusion of the precursor is about $\frac{1}{5}$ that for desorption and calculate the average number of hops the molecule takes before it either desorbs or dissociates. The simulations demonstrate that the precursor residence time and average diffusion distance *increase* with decreasing temperature. This result arises from the fact that although the diffusion rate decreases at lower temperatures the desorption rate decreases more rapidly so that the precursor makes on average more hops before desorbing. This leads to a larger island size at lower temperatures, which is opposite to the usual temperature dependence of island size found during MBE growth. We also investigated the effect of direct impingement and dissociation of the precursor without physisorption and diffusion. In this case, the differential dissociation probability due to the nature of the landing site is responsible for island growth. The simulations indicate that this mechanism should also lead to larger islands at lower temperatures, due to the autocatalytic effect.

At this time, the experimental evidence is insufficient to determine which of these two transport mechanisms is affecting morphology. It is difficult to identify the presence of a mobile precursor species because the same general trends are predicted from simulations (i.e., a larger average cluster size for autocatalytic growth and an increase in cluster size with decreasing temperature are predicted to occur with or without a mobile precursor species present). In addition, the STM data in this work show no obvious temperature dependence to the island morphology when comparing images at similar coverage

(Fig. 3). There is a marked change in the nucleation rate with temperature, as shown in Fig. 2. However, this is due to the activated precursor dissociation process, rather than an adsorption-diffusion-dissociation process. The lack of a temperature dependence for the island morphology in these experiments could be due to the rather large errors associated with measuring island size. Perhaps the mobile precursor is so weakly bound and the activation energy for diffusion sufficiently small that, over the limited temperature range studied here, effects due to precursor mobility are not resolvable.

Preliminary analysis of the simulated island size distributions suggests that there may be differences for the mobile precursor versus the direct impingement mechanism. Direct impingement results in continuous nucleation in uncovered areas of the substrate, while a mobile precursor mechanism results in a denuded zone around existing islands due to incorporation at island edges. This leads to a larger number of small islands for direct impingement and is the subject of future work.

To conclude, we have used STM to investigate the development of film morphology during Fe CVD. In the earliest stages of growth, layer morphology is characterized by formation of small clusters (possibly single atom clusters) with no preferential dissociation at Si steps. At higher coverages, Fe CVD growth results in a larger average cluster size. Comparisons of chemical vapor deposited films to those grown by PVD show that the CVD growth morphology cannot be explained by a random deposition or dissociation process. We conclude that morphology of CVD-grown films results from an autocatalytic effect, i.e., preferential dissociation of precursor molecules onto preexistant Fe clusters.

The authors thank Bruce Kellerman for helpful discussions and J. A. Knapp for the HIBS work used to measure film coverage. This work was supported by the U.S. Department of Energy under Contract No. DE-AC04-94AL85000.

*Present address: NSF Engineering Research Center for Advanced Electronic Materials Processing, North Carolina State University, Raleigh, NC 27695-7920.

[1] Y. W. Mo, J. Kleiner, M. B. Webb, and M. G. Lagally, Phys. Rev. Lett. **66**, 1998 (1991); Y. W. Mo, B. S. Swartzentruber, R. Kariotis, M. B. Webb, and M. G. Lagally, *ibid.* **63**, 2393 (1989).

[2] M. D. Johnson, C. Orme, A. W. Hunt, D. Graff, J. Sudijono, L. M. Sander, and B. G. Orr, Phys. Rev. Lett. **72**, 116 (1994).

[3] J. A. Stroscio and D. T. Pierce, Phys. Rev. B **49**, 8522 (1994); J. A. Stroscio, D. T. Pierce, and R. A. Dragoset, Phys. Rev. Lett. **70**, 3615 (1993).

[4] D. D. Chambliss and K. E. Johnson, Phys. Rev. B **50**, 5012 (1994).

[5] R. Q. Hwang, J. Schroder, G. Gunther, and R. J. Behm, Phys. Rev. Lett. **67**, 3279 (1991).

[6] G. S. Bales, A. C. Redfield, and A. Zangwill, Phys. Rev. Lett. **62**, 776 (1989), and references therein.

[7] W. L. Gladfelter, Chem. Mater. **5**, 1372 (1993).

[8] L. Kipp, R. D. Bringans, D. K. Biegelsen, L.-E. Swartz, and R. F. Hicks, Phys. Rev. B **50**, 5448 (1994).

[9] J. J. Boland, Phys. Rev. Lett. **67**, 1539 (1991); Surf. Sci. **261**, 17 (1992); Phys. Rev. B **44**, 1383 (1991).

[10] M. J. Bronikowski, Y. Wang, and R. J. Hamers, Abstracts Am. Chem. Soc. **207**, 284 (1994); M. J. Bronikowski, Y. J. Wang, M. T. McEllistrem, and R. J. Hamers, Surf. Sci. **298**, 50 (1993).

[11] D. S. Lin, E. S. Hirschorn, T. C. Chiang, R. Tsu, D. Lubben, and J. E. Greene, Phys. Rev. B **45**, 3494 (1992).

[12] J. A. Venables and G. L. Price, in *Epitaxial Growth,* edited by J. W. Matthews (Academic, New York, 1975), Pt. B.

[13] R. R. Kunz and T. M. Mayer, J. Vac. Sci. Technol. B **6**, 1557 (1988).

[14] For analysis of various carbonyl systems, see F. A. Houle and K. A. Singmaster, J. Phys. Chem. **96**, 10425 (1992).

[15] D. P. Adams, E. Chason, T. M. Mayer, and B. Kellerman (unpublished).

[16] J. R. Swanson, C. M. Friend, and Y. J. Chabal, J. Chem. Phys. **87**, 5028 (1987).

[17] J. S. Foord and R. B. Jackman, Surf. Sci. **171**, 197 (1986); Chem. Phys. Lett. **112**, 190 (1984).

[18] B. S. Swartzentruber, Y. W. Mo, M. B. Webb, and M. G. Lagally, J. Vac. Sci. Technol. A **8**, 210 (1990).

[19] Temperature calibration involved sinking a W/WRe thermocouple junction into an 0.008 in. diameter hole (~0.040 in. deep) drilled in the side of the Si samples.

[20] The pressure was measured by an uncalibrated ion gauge that was turned on only for the brief amount of time required for pressure equilibration (~30 sec).

[21] For a description of the HIBS technique, see J. A. Knapp and B. L. Doyle [Nucl. Instrum. Methods Phys. Res., Sect. B **45**, 143 (1990)] or B. L. Doyle, J. A. Knapp, and D. L. Buller [*ibid.* **42**, 295 (1989)].

[22] E. Chason and B. W. Dodson, J. Vac. Sci. Technol. A **9**, 1545 (1991).

[23] The energy for dissociation onto Fe was taken to be different for various n-Fe nearest neighbors (nn): $E_{act}(0\ \text{Fe nn}) = 0.4$ eV, $E_{act}(1\ \text{Fe nn}) = 0.25$ eV, $E_{act}(2\ \text{Fe nn}) = 0.19$ eV, $E_{act}(3\ \text{Fe nn}) = 0.13$ eV, and $E_{act}(4\ \text{Fe nn}) = 0.07$ eV.

[24] R. R. Kunz, T. E. Allen, and T. M. Mayer, J. Vac. Sci. Technol. B **5**, 1427 (1987).

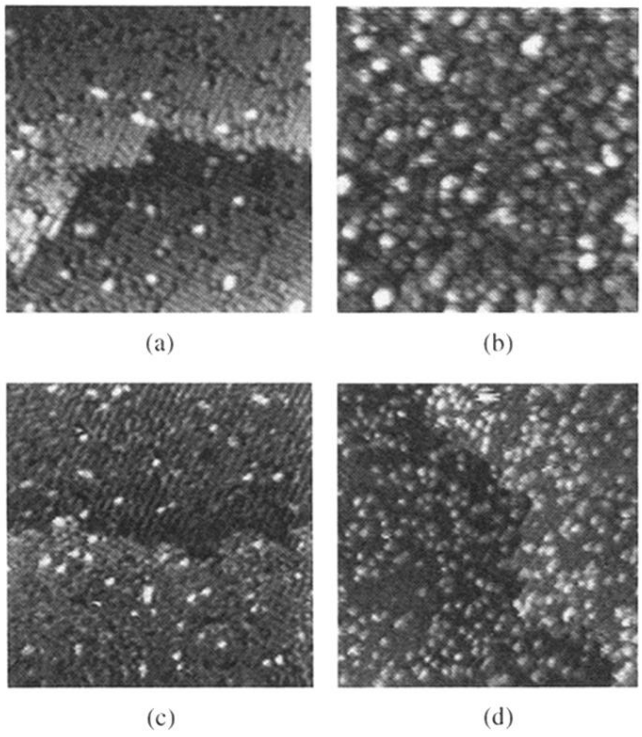

FIG. 1. 310 Å × 310Å STM images of Fe layers grown at 215 °C onto clean, reconstructed Si(100) by chemical vapor deposition [(a) and (b)] and Fe evaporation [(c) and (d)]. All images were taken using a bias of −2.5 V and a tunneling current of 0.15 nA.